Identification of potential sources and transport pathways of atmospheric PM_{10} using HYSPLIT and hybrid receptor modelling in Lanzhou, China

N. Liu[1,2], Y. Yu[1], J. B. Chen[1], J. J. He[1,2] & S. P. Zhao[1,2]
[1]*Key Laboratory of Land Surface Process and Climate Change in Cold and Arid Regions, Cold and Arid Regions Environmental and Engineering Research Institute, Chinese Academy of Sciences, Lanzhou, Gansu, China*
[2]*GraduateUniversity of Chinese Academy of Sciences, Beijing, China*

Abstract

Three-dimensional 4-day backward trajectories arriving at Lanzhou 500m above ground level were calculated every 6 h using HYSPLIT-4 trajectory model for spring (March, April and May) 2001 to 2008. The 8 years were divided into two categories: high dust years (2001, 2002, 2004 and 2006) and low dust years (2003, 2005, 2007 and 2008). Cluster analysis, potential source contribution function (PSCF) model, and concentration-weighted trajectory (CWT) method were used to evaluate the transport pathways and potential source regions affecting PM_{10} loadings in Lanzhou in spring season. Results indicate that the western and the northwestern pathways, accounting respectively 33% and 19.4% of all trajectories, were major pathways leading to high springtime PM_{10} loadings in Lanzhou during high dust years. However, the major pathways were the western and the northern pathways in low dust years, accounting for 23.6% and 18%, respectively. There were six potential source regions affecting PM_{10} concentration in Lanzhou, *e.g.* the Tarim Basin and the Turpan Basin in Xinjiang, the Qaidam Basin in Qinghai, the Hexi Corridor in Gansu province, the desert and Gobi areas in the middle and west of Inner Mongolia, and the Loess Plateau in the middle of Shaanxi province and eastern Sichuan.

Keywords: HYSPLIT, PM_{10}, trajectories, transport pathways, potential sources.

WIT Transactions on Ecology and the Environment, Vol 147, © 2011 WIT Press
www.witpress.com, ISSN 1743-3541 (on-line)
doi:10.2495/AIR110061

1 Introduction

With the rapid economic growth and accelerating urbanization, the primary pollutant in most Chinese urban areas has changed from SO_2 and TSP (Total Suspended Particles) to PM_{10} (aerosol particles with an aerodynamic diameter less than 10μm). PM_{10}, as atmospheric aerosols, affects the Earth's climate directly by absorbing or scattering solar and terrestrial radiation, and indirectly by altering cloud formation, microphysical properties, and lifetimes, [1, 2].

In East Asia, high PM_{10} loadings could arise from natural processes, *e.g.* surface dust, sea spray, and volcanic dust *etc*., anthropogenic activities, [2, 3], *e.g.* the combustion of fossil fuels and industrial production activities *etc*., and secondary aerosol particles. Dust storms occurring in the desert and Gobi desert in Central Asia and the northern regions of China, are not only a major weather phenomenon influencing the springtime climate in East Asia, but also a main source of atmospheric particles in spring in China. The desert areas in China, which occupy approximately 13% of China's land area, are major sources of Asian dust. A large number of observations and studies have shown that dust storms in Asia could not only increase the atmosphere aerosol concentrations in the local and adjacent areas, but also transport to the eastern parts of China, Korea, Japan and even across the Pacific to North America, [4–6].

Lanzhou, located in the northwest arid and semi-arid regions of China, is one of the most polluted cities in China. The PM_{10} concentrations in spring are dramatically affected by dust storms, [7]. Most of the previous studies on air pollution in Lanzhou were focused on the temporal variability of pollutants, [8], local transport and dispersion characteristics of pollutants, [9], the impact of dust weather, [10, 11], and control measurements, [12, 13], with little or no studies on the transport pathways and the source regions that affect air quality in Lanzhou. In order to control air quality, pollution sources must be identified, emission estimates made, and effective management strategies developed. Many studies have shown the signification correlation of the spatial and temporal variation of pollutants, including PM_{10}, [7], mercury, [14, 15], pollen, [16], and dust outbreak, [17], with air mass transport pathways. Hybrid receptor modeling, such as potential source contribution function (PSCF) model and concentration-weighted trajectory (CWT) method, has been used successfully for potential source region identification for PM_{10} and TGM (total gaseous mercury), [14, 18].

This research aims at identifying the transport pathways and the potential source regions that lead to elevated PM_{10} concentrations in Lanzhou and quantifying the relative contribution of the source regions to the PM_{10} loadings during spring (March, April and May) of 2001-2008. The results from this research would not only provide some scientific basis for improving the air quality in Lanzhou and the ecological environment of the surrounding regions, but also accumulate some experience for cities with similar situation in the world.

2 Data

The PM_{10} concentration data for Lanzhou in spring 2001 to 2008 were calculated from the air pollution index (API) reports for major Chinese cities, [19]. The process used to calculate PM_{10} concentrations from the API has been described in Zhang *et al.* [20].

The dust storm records (daily) were obtained from the Meteorological Administration of Gansu Province for the spring 2001 to 2008. The NCEP/NCAR (National Centers for Environmental Prediction and the National Center for Atmospheric Research) Reanalysis archive data were used as meteorological input data for trajectory calculations. The horizontal resolution of the data are 2.5°×2.5°in latitude and longitude, which are archived four times every day (00, 06, 12, 18 UTC).

3 Methods

3.1 Trajectory clustering analysis

Three-dimensional 4-day backward trajectories arriving at Lanzhou (Lat: 36.05N, Lon: 103.85E, 1518m above sea level) 500m above ground level (AGL) were calculated every 6 h (00, 06, 12, 18 UTC) using the National Oceanic and Atmospheric Administration (NOAA) HYSPLIT-4 (Hybrid Single-Particle Lagrangian Integrated Trajectory) model, [21], for the spring 2001 to 2008. The eight years were divided into two categories, *i.e.* high dust years with more than 6 dust storms in spring (2001, 2002, 2004 and 2006) and low dust years (2003, 2005, 2007 and 2008). The final model outputs were hourly backward trajectory endpoints indicating the geographical location and the height of the air parcel. Ward's hierarchical clustering method was used for all the eight spring seasons based on the mean angle between all pairs of trajectories, [7, 22]. The major transport pathways leading to the elevated PM_{10} concentrations in Lanzhou during spring could be obtained by combining the trajectory with the daily PM_{10} concentration data.

3.2 Potential source contribution function (PSCF)

A potential source contribution function (PSCF), [23], was used to identify the potential source regions that affect the PM_{10} loadings during springtime in Lanzhou. The PSCF values for the grid cells in the study domain were calculated by counting the trajectory segment endpoints terminating within each cell. By defining the number of endpoints that fall in the ijth cell as n_{ij} and the number of endpoints that corresponds to a PM_{10} concentration above an arbitrarily set criterion when arriving at Lanzhou in the same grid cell as m_{ij}, the PSCF value for the ijth cell can be defined as:

$$PSCF_{ij} = m_{ij} / n_{ij} . \quad (1)$$

Thus, the PSCF value can be interpreted as a conditional probability describing the potential contributions of a grid cell to the high PM_{10} loadings in

Lanzhou. That is, grid cells related to high PSCF values are the potential source regions, and the trajectories passing these cells are the major transport pathways leading to high PM_{10} loadings during spring in Lanzhou. In this study, the spring time daily-averaged PM_{10} concentration is used as the criterion for counting m_{ij}. To reduce the uncertainty of PSCF resulted from small n_{ij} values, an arbitrary weight function W_{ij} is multiplied to the PSCF value to better reflect the uncertainty in the values for cells with small n_{ij}. The weight function W_{ij} is defined as follows, [7],

$$W_{ij} = \begin{cases} 1.00, 40 < n_{ij} \\ 0.70, 10 < n_{ij} \le 40 \\ 0.42, 5 < n_{ij} \le 10 \\ 0.17, n_{ij} \le 5 \end{cases}. \tag{2}$$

The weight function reduced the PSCF value when the total number of endpoints in a particular cell was less than about three times the average value of the endpoints per cell (about 40 in this study), [24].

In this study, geographic areas covered by more than 95% of the backward trajectories were selected as the study domain. For the springtimes in high dust years (2001, 2002, 2004 and 2006), the study domain extends from 55° E to 125° E and from 25° N to 65° N, thus composing 11,200 cells 0.5° × 0.5° in latitude and longitude. The total number of trajectory endpoints located in the study domain is 142,784 so there would be about 13 endpoints per cell on average. That is, it is necessary to reduce the uncertainty of PSCF values by using eqn. (2) when the number of trajectory endpoints n_{ij} in a grid cell is less than about 40.

3.3 Concentration-weighted trajectory (CWT) method

One limitation of the PSCF method is that grid cells may have similar PSCF values when PM_{10} concentrations at the receptor site are either only slightly or extremely higher than the average value in spring. The PSCF value can only give the spatial distribution of potential source regions and cannot give information on the relative contribution of different potential source regions. To compensate the limitation, a concentration-weighted trajectory (CWT) method, [18, 25], was used to calculate the trajectory weighted concentration. In the CWT method, each grid cell is assigned a weighted concentration by averaging the sample PM_{10} concentrations that have associated trajectories crossing the grid cell as follows:

$$C_{ij} = \frac{1}{\sum_{l=1}^{M} \tau_{ijl}} \sum_{l=1}^{M} C_l \tau_{ijl} \tag{3}$$

where C_{ij} is the average weighted concentration in the ijth cell, l is the index of the trajectory, C_l is the PM_{10} concentration measured on the arrival of trajectory l, M is the total number of trajectories, and τ_{ijl} is the time spent in the ijth cell by trajectory l, [18]. The eqn. (2) was also applied to the calculation of CWT to reduce the uncertainties when n_{ij} is small. A high C_{ij} value implies that air

parcels traveling over the *ij*th cell would be associated with high PM_{10} concentration at the receptor site Lanzhou.

4 Results and discussion

4.1 PM_{10} pollution in spring

The occurrence of dust storms during springtime 2001 to 2008 in Lanzhou is summarized in table 1. According to the number of dust storm events, years 2001, 2002, 2004 and 2006 are classified as high dust years and years 2003, 2005, 2007 and 2008 are classified as low dust years.

Table 1: Occurrence of dust storms in spring during 2001–2008.

Year	2001	2002	2003	2004	2005	2006	2007	2008
Dust events (num)	15	9	6	11	2	12	5	4

The springtime daily-averaged PM_{10} concentration for Lanzhou is 238.8μg/m^3 in high dust years (fig. 1) and there are 138 days with daily PM_{10} concentrations higher than the average. The daily-averaged PM_{10} concentration is 157.2μg/m^3 in low dust years (fig. 2) and there are 123 days with higher than average PM_{10} concentrations. The daily-averaged PM_{10} concentration for the four spring seasons in high dust years is much higher than the national Grade II

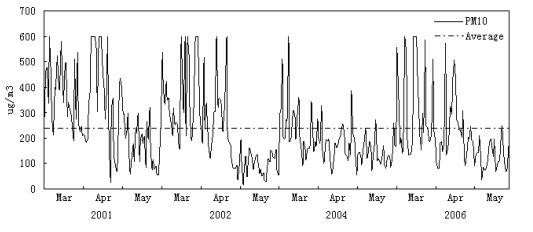

Figure 1: Daily-averaged PM_{10} mass concentrations at Lanzhou in spring for the years 2001, 2002, 2004 and 2006.

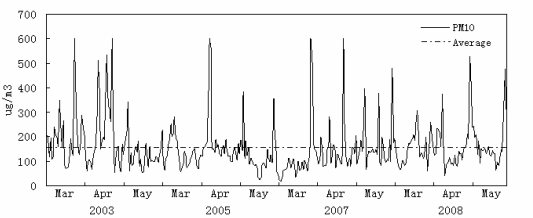

Figure 2: Same as fig. 1 but for the years 2003, 2005, 2007 and 2008.

standard for daily mean PM_{10} concentration of 150μg/m^3 (GB3095-1996), while it is slightly higher than the Grade II standard in low dust years. The averages in both categories exceed the Grade II standard by 67.7% and 38.0%, respectively. In addition, there are 51 days (accounted for 13.9%) and 13 days (accounted for 3.5%) when the national Grade V PM_{10} standard of 420μg/m^3 were exceeded during the spring of the high and the low dust years, respectively.

4.2 Cluster-mean backward trajectories

4.2.1 Transport pathways of mean backward trajectories

Seven clusters (1 to 7) were produced by the clustering algorithm for the high dust years, and the cluster-mean trajectories are shown in fig. 3(a). Six clusters (1 to 3 and 5 to 7) were obtained for the low dust years (fig. 3(b)). The transport routes and the direction of trajectories indicate the geographical areas traveled by air masses before their arrival at the receptor site. The length of the cluster-mean trajectories indicates the transport speed of air masses. The longer is the cluster-mean trajectory, the faster is the air mass. It is seen from fig. 3 that the western and the northwestern trajectories (cluster 2 and cluster 3) were longer than trajectories from other directions, indicating that air masses from the west and the northwest moved faster than others.

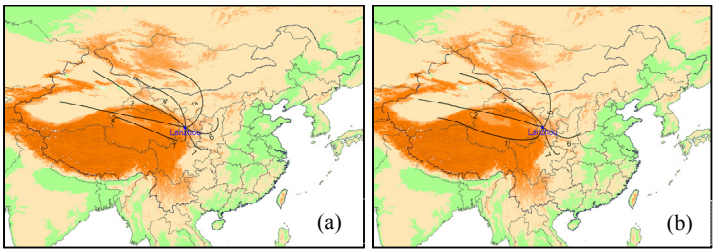

Figure 3: Cluster-mean back-trajectories arriving at Lanzhou in spring for (a) 2001, 2002, 2004 and 2006 (b) 2003, 2005, 2007 and 2008.

In high dust years, the air mass associated with cluster 1 were from western China, including the north Qinghai-Tibet Plateau, and the Gobi desert around the Qinghai and Xinjiang border. These trajectories moved southeasterly over the Qaidam basin and the border areas of Sichuan and Gansu province, and then turned northerly to Lanzhou. The air masses associated with clusters 2 and 3 were from Xinjiang province. The Cluster 2 air masses were from the Tarim Basin in southern Xinjiang; these trajectories passed the Taklimakan desert, and then moved westerly over the Qaidam Basin in northern Qinghai before arriving at Lanzhou. The Cluster 3 air masses were from the Junggar Basin, north of Xinjiang province; these trajectories moved southeasterly into the Gansu province and travelled along the Hexi Corridor to Lanzhou. The air masses associated with clusters 4 and 5 were initially from the desert, semi-desert and Gobi regions of Mongolia. The cluster 4 air masses moved from the southwestern Mongolia and travelled southeasterly over the Badain Jaran Desert

in the west of Inner Mongolia to Lanzhou; in contrast, the cluster 5 moved from the middle of Mongolia and travelled southerly to the middle of the Inner Mongolia, then passed through the Tengger Desert and finally turned southwesterly to Lanzhou. The air masses associated with clusters 6 and 7 were from the Loess Plateau and the border regions between Shaanxi and Sichuan province, respectively.

The six clusters in the low dust years are denoted following the high dust years for easy comparison. In the low dust years, the air masses associated with cluster 1 were from the marginal regions south of the Tarim Basin, these trajectories moved westerly through the neighboring regions of Xinjiang, Qinghai and Tibet and crossed the south of Qinghai province, and then turned northerly to Lanzhou. The air masses associated with cluster 3 in the low dust years were from the Junggar Basin, north of Xinjiang province, same as the cluster 3 in the high dust years, but the part of pathway within the Gansu province was different. The air masses associated with cluster 3 in low dust years moved southeasterly over the desert and Gobi desert regions near the border of the Inner Mongolia and the Gansu province to Lanzhou. The trajectories in cluster 5 in low dust years moved over Inner Mongolia and directed to Lanzhou without passing through the Ningxia province, which is different from the one in high dust years. The air masses associated with cluster 6 traveled more southerly in low dust years than the corresponding one in high dust years. The air masses associated with cluster 7 were from Sichuan province in low dust years, as in high dust years, but located more southerly.

4.2.2 Transport pathways of the polluted trajectories

All the backward trajectories were divided into two groups, *i.e.* the polluted and the clean trajectories, according to the sample PM_{10} concentration when they arrived at the receptor site. The polluted trajectories are those with PM_{10} concentrations higher than the average in spring seasons, *i.e.* 238.8μg/m^3 and 157.2μg/m^3 for the high and the low dust years, respectively. The number of trajectories, the percentage and the corresponding daily PM_{10} concentrations in each cluster for all trajectories and for polluted trajectories are summarized in tables 2 (for high dust years) and 3 (for low dust years).

In high dust years, the average PM_{10} concentrations of clusters 2 (287.7μg/m^3) and 3 (275.5μg/m^3) exceed the spring season average 238.8 μg/m^3, with more than 50% of trajectories being polluted ones, which indicates that the air masses associated with these clusters would carry more particulate matters and lead to high PM_{10} loadings in Lanzhou in high dust years. The clusters 2 and 3 represent the western and the northwestern pathways, which passed through major Asian dust source areas, therefore these two pathways, were major pathways carrying dust to Lanzhou. In comparison, fewer trajectories were assigned to clusters 1, 5, and 6 and the corresponding PM_{10} concentrations are lower than the spring season average, thus these clusters had less effect on PM_{10} loadings in Lanzhou. Cluster 7 was not a major transport pathway as no dust sources lie along the route. In high dust years, the pathways represented by

clusters 2 and 3 were polluted pathways, while clusters 1, 5, 6 and 7 were relatively clean pathways.

In low dust years, about 23.6% of trajectories were assigned to cluster 2, of which 44.0% were polluted trajectories. Cluster 2 represents the most important transport pathways with the highest PM_{10} concentration (177.1μg/m^3) among the six clusters. The second important transport pathway was associated with cluster 5, which had the second high PM_{10} concentration (170.1μg/m^3) and a relatively high percent of polluted trajectories (33.2%). The corresponding average PM_{10} concentrations of the two pathways, *i.e.* the western and the northern pathways, represented by clusters 2 and 5, exceeded the spring season average of 157.2 μg/m^3. These results indicate that air masses associated with clusters 2 and 5 would carry more particulate matters to Lanzhou and lead to high PM_{10} loadings in low dust years. The third important pathway was associated with cluster 3. Although 47.8% of the trajectories in cluster 1 were polluted, the number of trajectories assigned to the cluster is small, therefore, the pathway represented by cluster 1 was considered less important for PM_{10} loadings in Lanzhou. The pathways represented by clusters 2, 5 and 3 were polluted pathways, while clusters 1, 6 and 7 were relatively clean pathways in low dust years.

Table 2: Trajectory number and averaged PM_{10} concentration of each cluster for high dust years 2001, 2002, 2004 and 2006.

	All trajectories			Polluted trajectories*		
Cluster	Number	Percent of total	PM_{10} concentration (μg/m^3)	Number	Percent of total	PM_{10} concentration (μg/m^3)
1	87	5.9	218.1±113.4	21	24.1	381.0±111.1
2	486	33.0	287.7±150.3	256	52.7	399.0±121.8
3	286	19.4	275.5±166.1	148	51.7	402.2±132.5
4	190	12.9	213.3±149.5	61	32.1	389.6±136.7
5	147	10.0	179.9±146.3	29	19.7	431.0±136.1
6	117	7.9	150.5±88.0	11	9.4	362.6±68.5
7	159	10.8	184.8±90.9	26	16.4	342.5±85.8

*Trajectories associated with those concentrations higher than the average (238.8 μg/m^3).

Table 3: Same as table 2 but for low dust years 2003, 2005, 2007 and 2008.

	All trajectories			Polluted trajectories*		
Cluster	Number	Percent of total	PM_{10} concentration (μg/m^3)	Number	Percent of total	PM_{10} concentration (μg/m^3)
1	161	10.9	171.6±90.2	77	47.8	235.0±91.9
2	348	23.6	177.1±112.5	153	44.0	255.8±129.5
3	255	17.3	148.9±88.6	78	30.6	247.3±98.4
5	265	18.0	170.1±133.2	88	33.2	312.6±142.4
6	162	11.1	126.3±88.3	33	20.4	259.6±111.8
7	281	19.1	137.3±62.3	63	22.4	224.8±72.5

*Trajectories associated with those concentrations higher than the average (157.2 μg/m^3).

4.3 Potential source regions and their relative contribution

The distributions of PSCF for high and low dust years are shown in fig. 4. In high dust years (fig.4 (a)), cells with high PSCF values appeared mainly in Xinjiang, Qinghai and Gansu provinces, that is, the potential source regions most likely to have effect on high PM_{10} concentration in springtime in Lanzhou were located in the Tarim Basin and the eastern Turpan Basin in Xinjiang province, the Qaidam Basin in Qinghai and the Hexi Corridor in Gansu. The air masses from these potential source regions traveled along the pathways represented by clusters 2 and 3 to Lanzhou. In low dust years (fig. 4 (b)), cells related to high PSCF values were located in the Tarim Basin in Xinjiang, the Qaidam Basin in Qinghai, the degradated grassland near the borders of Qinghai, Sichuan and Gansu provinces, and the desert and Gobi desert in central and western Inner Mongolia. The air masses from these potential source regions traveled along pathways represented by clusters 1, 2 and 5 to Lanzhou. The effect of potential source regions on PM_{10} loadings in Lanzhou is lower in low dust years than that in high dust years.

Fig. 5 shows the distribution of weighted trajectory concentrations which gives the information on the relative contribution of potential source regions to PM_{10} loadings in Lanzhou. The potential source regions that are represented by

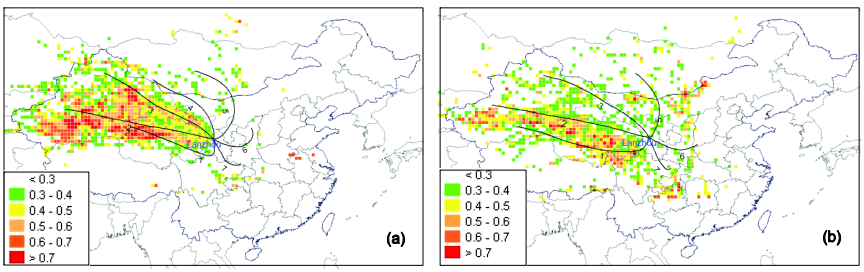

Figure 4: Potential source contribution function map of PM_{10} in spring during (a) 2001, 2002, 2004 and 2006, (b) 2003, 2005, 2007 and 2008. Darker colors indicate greater potential source.

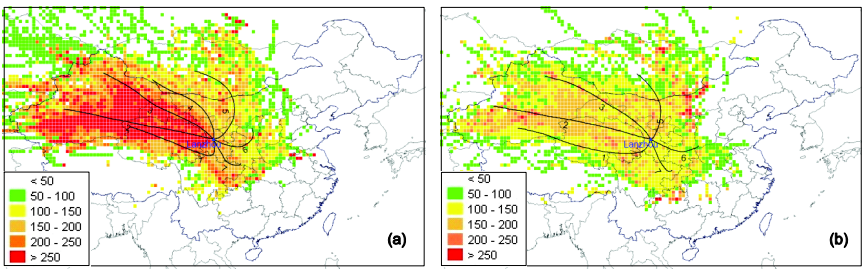

Figure 5: Concentration-weighted trajectory method analysis map of Lanzhou in spring during (a) 2001, 2002, 2004 and 2006, (b) 2003, 2005, 2007 and 2008. Darker colors indicate greater influence.

CWT values higher than 250μg/m^3 (fig. 5(a)) include the Tarim Basin and the Turpan Basin in Xinjiang, the deserts near the border of Xinjiang and Gansu, the Qaidam Basin in Qinghai, and the Hexi Corridor in Gansu. In low dust years (fig. 5(b)), the potential source regions are mainly located in the southern Taklimakan Desert and the Gobi Desert in eastern Xinjiang, the Gobi Desert in central and western Inner Mongolia and the Qaidam Basin in Qinghai. The contribution of these potential source regions to the PM_{10} loadings in Lanzhou was 150μg/m^3 to 200μg/m^3 in low dust years.

The PSCF and CWT analyses give somewhat different results for Lanzhou. Compared to the PSCF results (fig. 4(a)), CWT results (fig. 5(a)) give more detailed information on source regions. For example, three more source regions can be seen in the CWT results, *i.e.* the Gobi Desert in Inner Mongolia, the Losses Plateau, and the western Sichuan and regions between Shaanxi and Gansu. The former two regions were not the major potential source regions as they had less affect on the PM_{10} loadings in Lanzhou. The third regions correspond to the "southerly sources" in Wang *et al.* [7]. The distribution of source regions in low dust years was similar to that in high dust years. Compared to the PSCF results (fig. 4(b)), the CWT results (fig. 5(b)) reveal more source regions, *e.g.* the Tengger Desert, the edge of the Gurbantunggut Desert, the northwestern Gansu and Qinghai, the Gobi Desert in Inner Mongolia and the borders of Sichuan, Gansu and Shaanxi.

5 Conclusion

The atmospheric pathways, potential source regions and their relative contribution to the high PM_{10} loadings in Lanzhou were identified by trajectory clustering techniques, potential source contribution function (PSCF) model, and concentration-weighted trajectory (CWT) method. Results indicate that the western and the northwestern pathways, accounting respectively 33% and 19.4% of all trajectories, were major pathways leading to high springtime PM_{10} loadings for Lanzhou in high dust years. However, the most important and the second important pathways were the western and the northern pathways in low dust years. In high dust years, the potential source regions were mainly located in the Tarim Basin and the Turpan Basin in Xinjiang, the border regions between Qinghai and Gansu, and the Hexi Corridor. In low dust years, the potential source regions were the Tarim Basin and the Turpan Basin in Xinjiang and the border regions among Xinjiang, Qinghai and Gansu. There were also some moderate potential sources including the northerly source, the southerly source and the Loess Plateau source. The northerly source was mainly distributed in the desert and Gobi desert in Inner Mongolia, the southerly source was in the border regions of Sichuan, Gansu and Shaanxi, and the Loess Plateau source was in the central areas of Shaanxi province. Although the potential source regions are similar in the high and the low dust years, the transport pathways and the relative contribution to PM_{10} loadings in Lanzhou are different.

It should be emphasized that the current study was conducted for spring. More research are needed to provide more detailed scientific basis on improving

the air quality in Lanzhou, especially the transport pathways and source regions for winter pollutants need to be identified by combining event analysis with high-resolution numerical simulations.

Acknowledgement

This research was funded by the Chinese Academy of Sciences through the '100 Talent Project'.

References

[1] Intergovernmental Panel on Climate Change (IPCC). In: Houghton, J.T., et al., (eds), Climate Change 2001, Cambridge University Press, New York, 2001.

[2] Kim J., Yoon S.C. & Jefferson A., et al., Aerosol hygroscopic properties during Asian dust, pollution, and biomass burning episodes at Gosan, Korea in April 2001. Atmospheric Environment, 40(8), pp. 1550-1560, 2006.

[3] Chen L.L., Carmichael G.R. & Hong M.S., et al., Influence of continental outflow events on the aerosol composition at Cheju island, south Korea. Journal of Geophysical Research, 102, pp. 28551-28574, 1997.

[4] Duce R.A., Unni C.K. & Ray B.J., et al., Long-range atmospheric transport of soil dust from Asia to the tropical North Pacific: temporal variability. Science, 209, pp. 1522-1524, 1980.

[5] Uematsu M., Duce R.A. & Prospero J.M., et al., Transport of mineral aerosol from Asia over the North Pacific Ocean. Journal of Geophysical Research, 88, pp. 5342-52, 1983.

[6] Husur R.B., Tratt D.M. & Schichtel B.A., et al., Asian dust events of April 1998. Journal of Geophysical Research, 106, pp. 18317-18730, 2001.

[7] Wang Y.Q., Zhang X.Y. & Arimoto R., The contribution from distant dust sources to the atmospheric particulate matter loading at XiAn, China during spring. Science of the Total Environment, 368, pp. 875-883, 2006.

[8] Yu Y., Xia D.S. & Chen L.H., et al., Analysis of particulate pollution characteristics and its causes in Lanzhou, Northwest China. Environmental Science, 31(1), pp. 22-28, 2010.

[9] Chu P.C., Chen Y.C. & Lu S.H., Atmospheric effects on winter SO_2 pollution in Lanzhou, China. Atmospheric Research, 89, pp. 365–373, 2008.

[10] Wang S.G., Wang J.Y. & Zhou Z.J., et al., Regional characteristics of three kinds of dust storm events in China. Atmospheric Environment, 39(3), pp. 509-520, 2005.

[11] Wang S.G., Yuan W. & Shang K.Z., The impacts of different kinds of dust events on PM_{10} pollution in northern China. Atmospheric Environment, 40(40), pp. 7975-7982, 2006.

[12] Zhang L., Chen C.H. & Murlis J., Study on winter air pollution control in Lanzhou, China. Water, Air, and Soil Pollution, 127, pp. 351–372, 2001.
[13] Chu P.C., Chen Y.C. & Lu S.H., Afforestation for reduction of NO_X concentration in Lanzhou China. Environment International, 34, pp. 688–697, 2008.
[14] Xu X. & Akhtar U.S., Identification of potential regional sources of atmospheric total gaseous mercury in Windsor, Ontario, Canada using hybrid receptor modeling. Atmospheric Chemistry and Physics, 10, pp. 7073-7083, 2010.
[15] Ci Z.J., Zhang X.S. & Wang Z.W., et al., Atmospheric gaseous elemental mercury (GEM) over a coastal/rural site downwind of East China: Temporal variation and long-range transport. Atmospheric Environment, 45, pp. 2480-2487, 2011.
[16] Efstathiou C., Isukapalli S., & Georgopoulos P., A mechanistic modeling system for estimating large-scale emissions and transport of pollen and co-allergens. Atmospheric Environment, 45, pp. 2260-2276, 2011.
[17] Escudero M., Stein A.F. & Draxler R.R., et al., Source apportionment for African dust outbreaks over the Western Mediterranean using the HYSPLIT model. Atmospheric Research, 99, pp. 518-527, 2011.
[18] Seibert P., Kromp-Kolb H. & Baltensperger U., et al., Trajectory analysis of aerosol measurements at high alpine sites. In: Borrell P.M., et al., (eds), Transport and transformation of pollutants in the troposphere. Academic Publishing, Den Haag, pp. 689-693, 1994.
[19] Ministry of Environmental Protection of the People's Republic of China (MEP). Beijing, www.zhb.gov.cn/index.htm.
[20] Zhang X.Y., Gong S.L. & Shen Z.X., et al., Characterization of soil dust aerosol in China and its transport/distribution during 2001 ACE-Asia, 1. Network observations. Journal of Geophysical Research, 108, pp. 4261, 2003.
[21] Draxler R.P. & Hess G.D. & An overview of the HYSPLIT-4 modeling system for trajectories, dispersion, and deposition. Australian Meteorological Magazine, 47, pp. 295-308, 1998.
[22] Sirois A. & Bottenheim J.W., Use of backward trajectories to interpret the 5-year record of PAN and O_3 ambient air concentrations at Kejimkujik National Park, Nova Scotia. Journal of Geophysical Research, 100, pp. 2867-2881, 1995.
[23] Ashbaugh L.L., Malm W.C. & Sadeh W.Z., A residence time probability analysis of sulfur concentrations at Grand Canyon National Park. Atmospheric Environment, 19, pp. 1263-1270, 1985.
[24] Polissar A.V., Hopke P.K. & Harris J.M., Source regions for atmospheric aerosol measured at Barrow, Alaska. Environmental Science and Technology, 35, pp. 4214-4226, 2001.
[25] Hsu Y.K., Holsen T.M. & Hopke P.K., Comparison of hybrid receptor models to locate PCB sources in Chicago, Atmospheric Environment, 37, pp. 545-562, 2003.